High Resolution Spectroscopy of ^{10}Li

Takashi Nakamura, Ryuki Tanaka, and SAMURAI Collaboration[1]
Department of Physics, Tokyo Institute of Technology

Abstract

We propose to determine experimentally the low-lying states of ^{10}**Li**, which has long been controversial and crucial in discussing the Borromean structure of ^{11}Li, with the newly developed high-resolution neutron detector array HIME(**HI**gh resolution detector array for **M**ulti-neutron **E**vents), combined with the SAMURAI setup. The HIME is made up of 100 rods of 2x4x100cm^3 plastic scintillators, and can track the recoiled proton to improve the energy resolution. In this proposal we measure the relative energy $E_{\rm rel}$ spectrum of ^{10}Li (n+ ^{9}Li) in the breakup reaction of ^{11}Li, ^{11}Be, and ^{12}B. The use of different reaction channels can differentiate the spin-parity of the low-lying states in ^{10}Li.

1 Introduction

Unbound nuclei in the vicinity of the neutron drip line play an important role in nuclear physics since one of the ultimate goal of nuclear physics is to describe many-body nucleonic systems from the β-stability line to the drip-lines, and even *beyond*. Such nuclei are used to test modern nuclear structure theories, such as ab-initio calculations as well as Gamow shell models. It is also important to understand the Borromean nuclei since its constituent is a barely unbound nucleus, as in ^{10}Li in ^{11}Li, which is of the current interest of this proposal.

The experiment aims at measuring the ^{10}Li energy spectra with the highest energy resolution that has ever been achieved. The structure of ^{11}Li, including that of its constituent ^{10}Li, has been one of the high-lights since the discovery of the two-neutron halo Borromean structure in ^{11}Li. Since 2006, more precise data on ^{11}Li have been accumulated; the Coulomb breakup [1], the charge radius [2], the precise mass [3, 4], and the $p(^{11}\mathrm{Li},t)^9$Li transfer reaction [5], which have enhanced further interests in ^{11}Li and ^{10}Li. The binding mechanism of this Borromean system, the dineutron correlation, and the shell degeneracy of $\nu(1s_{1/2})^2$ and $\nu(0p_{1/2})^2$ (about 50% vs. 50% [6, 7]) have been investigated experimentally and theoretically. Recently, tensor-optimized shell model (TOSM) [8], which introduced the tensor correlation in the ^{9}Li core, has shed light on the mechanism of this degeneracy.

The unbound nucleus ^{10}Li has been of great importance in discussing the halo structure of ^{11}Li, and has been measured by many groups [9]. The current concensus of the energy levels of ^{10}Li is that there is a *single* s-wave virtual state of

[1]The Member list is attached in a separate sheet

the scattering length $a \sim -20$ fm, and a *single* p-wave resonance at about 500 keV above the ^{9}Li+n threshold, as summarized in Fig. 1. The charge exchange reaction ^{10}Be(^{12}C,^{12}N)^{10}Li showed the state at 0.24 MeV, which was assigned as another p-wave resonance (1^+)[11]. However this 0.2 MeV state has never been observed in the breakup experiments, and the low-lying states of ^{10}Li are thus still controversial.

Theoretically, a single p-wave (s-wave) peak, observed in most of the experiments, should be doublet since ^{10}Li is an odd-odd nucleus. The $0p_{3/2}$ proton coupled to the $0p_{1/2}$ neutron can make 1^+ and 2^+ states, while that coupled to the $1s_{1/2}$ neutron can make 1^- and 2^- states. For instance, the TOSM calculation by Myo *et al.* TOSM) predicted the doublets for these states as in Table 1[8]. It is interesting that the inert core of ^{9}Li leads to quite a different picture about ^{10}Li as shown in the Table.

As mentioned, most of the experiments failed to see the doublets, which may be attributed to a lack of the energy resolution. With enhanced beam intensity and high energy at RIBF, and current technology of neutron detection, we here aims at measuring the ^{10}Li spectrum with high precision and high statistics to disentangle the situation on the low-lying states of ^{10}Li.

We use the invariant mass method, where the unbound state ^{10}Li is first produced, and then momenta of all the decay particles ^{9}Li+n are measured to reproduce the invariant mass spectrum. We use the three reaction channels; ^{11}Be$\rightarrow$^{10}Li ($-1p$), ^{11}Li$\rightarrow$^{10}Li ($-1n$), and ^{12}B$\rightarrow$^{10}Li ($-2p$), each with a carbon target. The use of a different projectile is to select specific spin-parity states. ^{11}Be, whose ground state is dominated by the s-wave valence neutron configuration, is expected to lead to the s-wave states in ^{10}Li by the one-proton knockout. Meanwhile, the use of the ^{11}Li projectile, which is a mixture of $\nu(1s_{1/2})^2$ and $\nu(0p_{1/2})^2$, leads to both the p-wave and s-wave states in ^{10}Li. ^{12}B is expected to lead to the p-wave states.

In addition we can use the transverse momentum ($P_\perp$) of ^{10}Li in the $1n$ removal reaction of ^{11}Li. The $P_\perp$ distribution in combination with the $E_{\rm rel}$ spectrum, we can distinguish the orbital angular momentum of the valence neutron according to the states in ^{10}Li. This method is very useful, as shown in the experiment of the one neutron removal of ^{14}Be leading to the unbound state of ^{13}Be [12], where we found the intruder ground state of ^{13}Be for the first time.

We make use of a newly-developed high-resolution neutron detector array HIME which is to be combined with the SAMURAI setup to measure the invariant mass. As later described, the HIME can improve the energy resolution by more than a factor of two, compared to the previous measurements, thereby enabling us to disentangle the doublets. This will be the first experiment using the HIME array, which is the new-generation neutron detector arrays using the tracking of the recoil proton.

2 Experimental Method

We perform a kinematical complete measurement of the breakup reactions, ^{11}Be$\rightarrow$^{10}Li ($-1p$), ^{11}Li$\rightarrow$^{10}Li ($-1n$), and ^{12}B$\rightarrow$^{10}Li ($-2p$) on a carbon target at the energy of about 230-250 MeV/nucleon. We measure all the momenta of outgoing particles, ^{9}Li

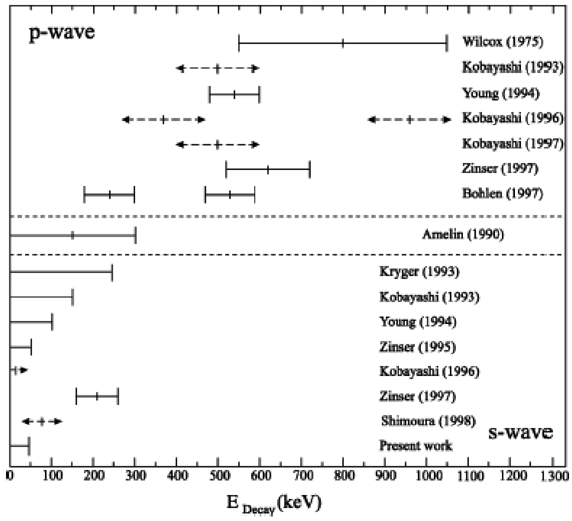

Figure 1: The summary of the experimental data for the energy levels of ^{10}Li with respect to the ^{9}Li+n decay threshold. The figure is obtained from Ref. [9]. The p-wave state at about 0.5 MeV and the s-wave virtual state are found in most of the experiments, while transfer(charge-exchange) experiments (BOHL97) shows the two p-wave states at 0.2 MeV and 0.5 MeV states.

	TOSM	Inert Core
$(E_r, \Gamma)(1^+)$ (MeV)	(0.22, 0.09)	(0.03,0.005)
$(E_r, \Gamma)(2^+)$ (MeV)	(0.64, 0.45)	(0.33,0.20)
$a_s(1^-)$ (fm)	-5.6	1.4
$a_s(2^-)$ (fm)	-17.4	0.8

Table 1: Theoretical estimations for the low-lying ^{10}Li states by Myo et al.[8]. The resonance energies E_r and the decay widths Γ of the p-wave resonance states (1^+ and 2^+) in ^{10}Li, and the scattering length of the s virtual states (1^- and 2^-). The TOSM takes into consideration the tensor and pair correlations in ^{9}Li, while the 'Inert Core' calculation assumes the inert core of ^{9}Li.

plus neutron for ^{10}Li measurements. The invariant mass is then reconstructed as,

$$M(^{10}\mathrm{Li}) = \sqrt{\left(E(^{9}\mathrm{Li}) + E(n)\right)^2 - \left(\vec{P}(^{9}\mathrm{Li}) + \vec{P}(n)\right)^2}. \tag{1}$$

Then, the relative energy E_{rel} can be extracted as

$$E_{\mathrm{rel}} = M(^{10}\mathrm{Li}) - M(^{9}\mathrm{Li}) - M(n), \tag{2}$$

When the outgoing ^{9}Li is in the excited state at 2.69 MeV, mass should be replaced by that of the excited state, which can be distinguished by a coincidence measurement of the γ ray.

In the ^{11}Li breakup, we also measure the transverse momentum of ^{10}Li in the rest frame of ^{11}Li. This can be realized by measuring ^{11}Li momentum, in addition.

2.1 Experiment

The experimental setup is shown in Fig. 3 and Fig. 4. The secondary beams are produced by the fragmentation of ^{18}O at 290 MeV/nucleon of about 500 pnA with a thick Be production target at the F0 focus of the BigRIPS (See Fig.3).

The secondary beam intensities are estimated to be over 10^6 cps for all the beams. However, we need to keep the beam rate as low as 10^5 cps due to the limitation of the beam detectors. We thus set the momentum slit to be very narrow ($\Delta P/P = \pm 0.22\%$ for ^{11}Li, and $\Delta P/P = \pm 0.03\%$ for ^{11}Be and ^{12}Be beams), which is good for obtaining the better beam quality. The beam purity for each run is basically 100% except for the ^{11}Li, where triton could be mixed. The secondary beam energies we use are listed in Table 2.

The particle identification of the projectile is performed by measuring the time of flight TOF, $B\rho$, and ΔE. The TOF is measured between the plastic scintillator at F3 and F7, or between F3 and SBT, where the SBT is the scintillator about 2 m upstream of the target (see Fig. 4). $B\rho$ is measured by the position information at F5 (dispersive focus), which can be obtained by the time difference of the two phototubes attached in the left and right side of the plastic scintillator. The ΔE is measured at the plastic scintillator at F7 (or SBT).

Following the breakup, we measure momentum vectors of the neutron and the charged fragment ^{9}Li in coincidence emitted in a narrow kinematical cone following the breakup of the projectile with the C targets, by the newly-developed neutron detectors HIME with the standard SAMURAI setup as shown in Fig. 4. The target thickness of C is chosen as shown in Table 2, to optimize the resolution and the yield.

The HIME is composed of 100 pieces of plastic scintillator modules, each of which is $100\times4\times2$ cm^3 in dimension and is coupled to two phototubes at both ends of the longest direction. This is arranged into 20 pieces $\times$ 5 layers as in Fig. 4. Since the direction of each layer is alternate by 90 degrees, the penetration of the second layer of the recoil proton can be used to extract the 3D hit position using the two bars which fire. The high granularity as in the present setup enhances the resolution. The penetration of three layers allow us to track the direction of the recoil proton, which improves further the resolution. The resultant energy resolution for the three-layer tracking is estimated to be less than or about 200 keV at $E_{\rm rel}$ =1 MeV in FWHM, i.e., 160keV, 180keV, 220keV for the beams of ^{11}Li, ^{11}Be, and ^{12}B, respectively, with the target thickness in Table 2. This is better by a factor of two, compared to the breakup measurement of ^{11}Li at 70 MeV/nucleon at RIPS (450 keV FWHM). The improvement of the resolutions can be seen in Fig. 2. The tracking efficiency which requires for a recoiled proton to penetrate at least three-layers of the HIME is 2.5%. Such a tracking analysis is necessary to obtain the resolutions mentioned.

The HIME is located at 8 m downstream of the target, and is installed such that the horizontal edge of the effective area of the HIME is on the beam axis, to optimize the acceptance. The acceptance curve is shown in Fig. 5, which is rather smooth in the region of the current most interest ($E_{\rm rel} \leq$ 1MeV).

We also use the NEBULA setup for the $2n$+^{9}Li coincidence events. The $2n$ detection events are used to estimate the background caused by the excitation of ^{11}Li, which decays into ^{9}Li+n+n, but only one neutron plus ^{9}Li is detected. Such a background becomes problematic when there is a strongly populated narrow resonance in ^{11}Li as in the case of ^{14}Be(2^+). The $2n$ detection efficiency for $E_{\rm rel}$=1 MeV is about 12%. The measurement with NEBULA also helps to estimate the acceptance curve in HIME (for ^{9}Li+n), since NEBULA has a much wider acceptance.

We also measure the γ ray, in coincidence with $1n$ and ^{9}Li with the NEBULA, DALI2, and the SAMURAI spectrometer, to determine if there is any ^{9}Li*($E_{\rm x}$ =2.69 MeV) configuration in a ^{10}Li state. We estimate that the γ ray efficiency of 7% for 2.7 MeV γ ray with the DALI2.

3 Estimation of beam time requested

Table 2 summarizes the intensities and evaluated event rates. Based on this, we request **5** days in total (excluding the 1-day secondary beam tuning), whose detail is shown in Table 3. In the case of the ^{11}Li beam, we aim to collect 80000 events, which will allow us to analyze in detail the ^{10}Li transverse momentum distribution as a function of relative energy by dividing the $E_{\rm rel}$ spectrum into 20 50 keV wide bins (0$\leq E_{\rm rel} \leq$1 MeV) with statistical uncertainty of some 7% for each bin. For the one-dimensional $E_{\rm rel}$ spectrum, we expect to obtain the statistics as in Fig. 2, which is sufficient to disentangle the p-wave doublets. For the ^{12}B and ^{11}Be projectile runs, we collect 6000 events each. since we primarily use only the $E_{\rm rel}$ 1D spectra for these projectiles.

We also would like to make a neutron calibration run using the mono-chromatic neutrons produced from the ^{7}Li(p,n) reaction for another 1 day.

4 Readiness

We plan to use the newly-developed HIME neutron array, combined with the standard SAMURAI setup. The SAMURAI is scheduled to be ready by Feb. 2012. The HIME

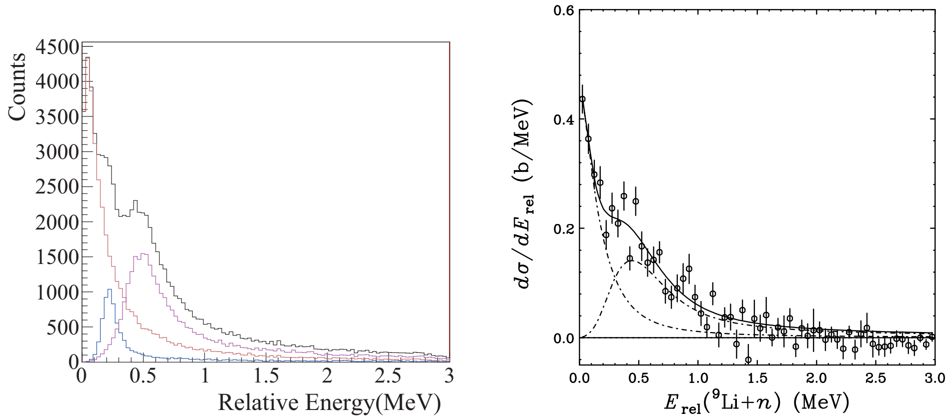

Figure 2: Left: Estimated $E_{\rm rel}$ spectra for ^{10}Li in a breakup of ^{11}Li (total 80000 events), assuming the s-wave virtual state ($a_s = -12.5$ fm) plus p-wave doublets at E_r=0.22 MeV (Γ =0.09 MeV) and E_r=0.53 MeV (Γ =0.45 MeV), with the HIME and SAMURAI setup. The doublet p-wave states can be distinguished. The assumed ratio of the population is 5:1:4 for the s-wave and two p-wave doublets (0.22 MeV,0.53 MeV), which reproduces roughly the spectrum on the right-hand side with a worsened resolution. Right: The ^{10}Li spectrum obtained in ^{11}Li breakup on a carbon at 69 MeV/nucleon in the RIPS experiment. The s virtual component and the single p-wave component is seen, but it could not separate the p-wave doublets even if it exists.

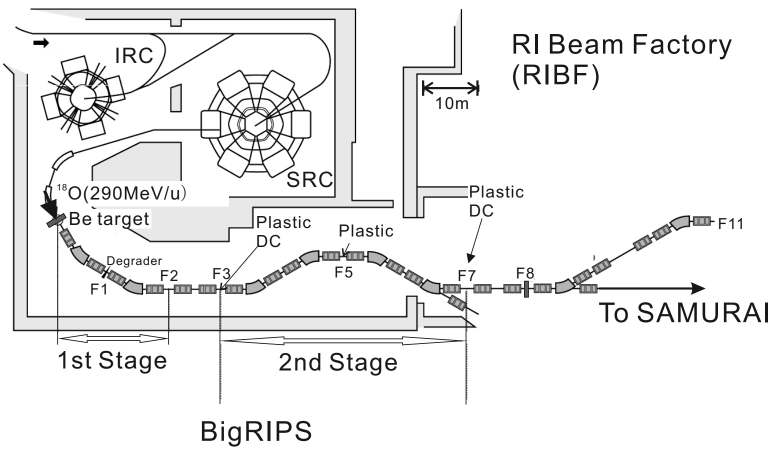

Figure 3: Layout of BigRIPS. For the beam counters, we primarily use F3,F5, and F7 plastic scintillators for the particle identification. MWPC's at F3 and F7 are used for tuning the beam.

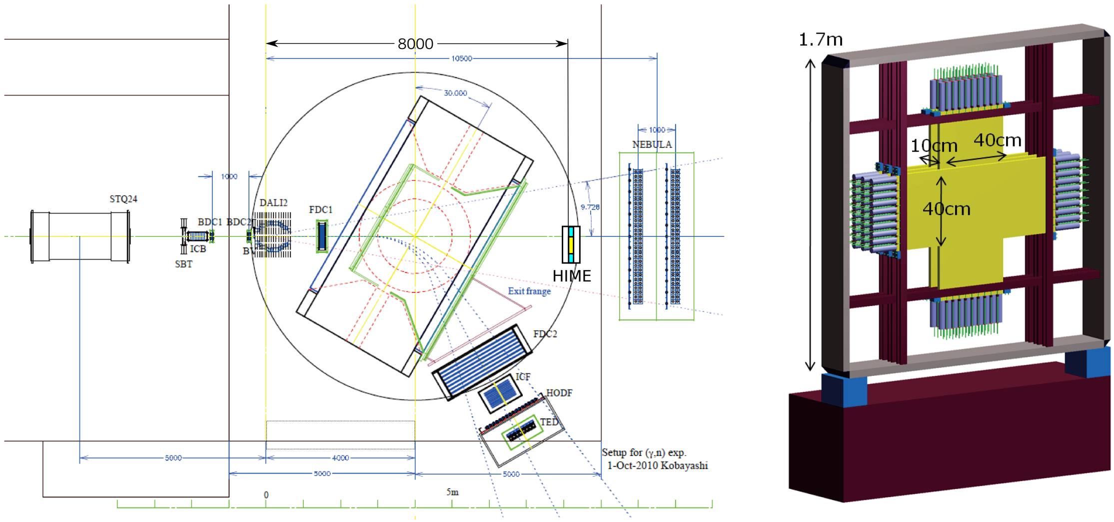

Figure 4: Experimental setup for the proposed experiment (ICB,ICF,TED are not used). The setup of HIME is also shown.

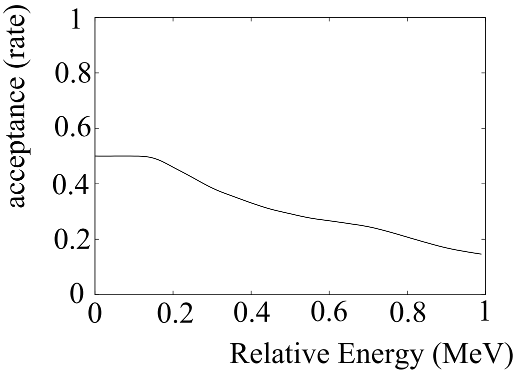

Figure 5: Acceptance estimated for the $1n$+^{9}Li coincidence events by the HIME setup with the SAMURAI as a function of $E_{\rm rel}(n+^{9}{\rm Li})$. The energy of the neutron is assumed to be 230 MeV, which is typical of the current measurement in ^{11}Li breakup.

Projectile	E/A(MeV)	$\Delta P/P$	t(g/cm^2)	Assumed σ_{-xN}	Y (cph)
^{12}B (HIME)	250	±0.03%	1	0.5 mb	5.5×10^1
^{11}Be (HIME)	256	±0.03%	1	10 mb	1.1×10^3
^{11}Li (HIME)	230	±0.22%	2	100 mb	2.2×10^4
^{11}Li (NEBULA,$2n$)	230	±0.22%	2	20 mb	8.6×10^3

Table 2: Estimated event rates for the $1n$ + ^{9}Li events with the HIME with SAMURAI, and for the $2n$+^{9}Li events with the NEBULA with SAMURAI.

Reaction	N-detector	Target-in	Target-out	Total
^{12}B $(-2p)$	HIME	60h	10h	70h
^{11}Be $(-1p)$	HIME	6h	1h	7h
^{11}Li $(-1n)$	HIME	4h	1h	5h
^{11}Li $(-1n)$	NEBULA	1.5h	0.5h	2h
Total				3.5d
Neutron Calib.				1d
Other Calib.				0.5d
				5 days

Table 3: Days to be requested based on the estimated beam intensity and event rates.

neutron detector array is now being constructed and ready by the end of the fiscal year 2011. In summary, we request 5-day machine time to perform the high-resolution measurement of ^{10}Li, as the first experiment for the HIME neutron-detector array.

References

[1] T. Nakamura *et al.*, Phys. Rev. Lett. **96**, 252502 (2006).

[2] R. Sanchez *et al.*, Phys. Rev. Lett. **96**, 033002 (2006).

[3] C. Bachelet *et al.*, Phys. Rev. Lett. **100**, 182501 (2008).

[4] M. Smith *et al.*, Phys. Rev. Lett. **101**, 202501 (2008).

[5] I. Tanihata *et al.*, Phys. Rev. Lett. **100**, 192502 (2008).

[6] H. Simon *et al.*,, Phys. Rev. Lett. **83**, 496 (1999).

[7] N. Aoi *et al.*, Nucl. Phys. A **616**, 181c (1997).

[8] T. Myo *et al.*, Prog. Theo. Phys. **119**, 561 (2008).

[9] M. Thoennessen *et al.*, Phys. Rev. C **59**, 111 (1999), and references therein.

[10] D.R. Tilley, et al., Nucl. Phys. A **745**, 155 (2004), and references therein.

[11] H.G. Bohlen, Prog. in Part. and Nucl. Phys. **42**, 17 (1999).

[12] Y. Kondo, T. Nakamura *et al.*, Phys. Lett. B **690**, 245 (2010).